Tidal modelling in the west coast of India

L. Testut[(1)(2)], A. Unnikrishnan [(2)]
(1) LEGOS, 14 Av. Edouard Belin 31400 Toulouse.
(2) NIO, Goa, India

Global tidal solutions are sometimes inaccurate in coastal regions. This is particularly true in some regions of the northern Indian Ocean, which are characterized by wide continental shelves and large tidal ranges. We show that these global solutions are inaccurate on the shelf region off Mumbai, off the west coast of India. In this region, the shelf is very wide and it opens into the Gulf of Khambhat, where large tides are observed. Moreover, it is noticed that in regions of large semi-diurnal tides in the Bay of Bengal, such as, the head Bay, Gulf of Martaban etc., global tidal solutions are not accurate. In the present work, we focus on the shelf region off the west coast of India. We used a new approach in developing a high resolution hydrodynamic tidal model for the inner shelf region (8° N to 22° N). The open boundary of the model is aligned to the altimetry tracks, which allowed to prescribe boundary conditions obtained directly from observations. It is shown that the tidal solutions at the coast are much improved compared to those obtained from the global solutions and that on the wide shelf portion and the Gulf of Khambhat the improvement has been considerable.

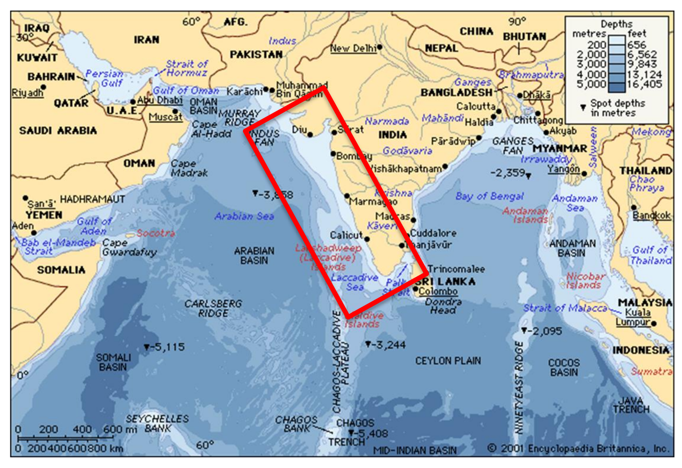

Figure 1: Modelled region

Model Set-Up

The hydrodynamic model used is the 2D barotropic shallow water module of the Toulouse *Unstructured* Grid Ocean model (T-UGOm) for its time-stepping mode and of the FES tidal solution (Lyard *et al.*, 2006) for its spectral mode. The tidal equations are derived from the classical non-linear shallow water equations (Lynch and Gray, 1979). The spectral and finite element characteristics of this model has proved to be the keys factor of the success of the FES atlases at global scale.

For the present work, we implemented a high resolution version of the T-UGOm model on the inner shelf along the western coast of India (Figure 2). The finite element mesh is composed of more than **15000 nodes** with the mesh element size ranging from less than a **1 km** at the coast to a maximum of **20 km** in the middle of the shelf. The model domain is essentially located on the shelf region at depth less than 200 m. Based on a sensitivity analysis we chose the improved bathymetric data (Sindhu *et al.*, 2007), which was developed by merging global bathymetry with information on depths in shallow regions derived from the hydrographic charts published by the Indian Naval Hydrographic Office. The open boundary tidal conditions were taken from the new **CTOH** tidal constants product (http://ctoh.legos.obs-mip.fr/products/coastal-products/coastal-products-1/tidal-constants). This product contains along-track estimates of amplitude and phase lag for the major tidal constituents which are derived from the harmonic analysis of along-track observations from different altimetric missions (TOPEX/Poseidon, JASON 1&2). The open boundary conditions were prescribed using information at 319 points, extracted from altimetry track 66 and 79 (see Figure 2). The model was then forced with altimetry-derived elevation (amplitudes and phases) from 21 tidal constituents (M2, K2, S2, 2N2, MU2, N2, NU2, T2, K1, O1, OO1, P1, Q1, J1, M1, M4, MS4, MF, MM, MTM, SSA). The reference simulation is performed using a quadratic bottom friction (C_D=1.6x10^{-3}) with the parameterization of the internal drag switch off. The numerical times needed for the spectral simulation to iterate over the tidal constituents is usually within few minutes.

The main database used for the validation purpose is the tidal harmonic constants (amplitude and phase) based on the Admiralty Tide Tables (ATT, 1996). Out of the 136 stations available in this database for the west coast of India, 66 fall inside the model domain. Among these 66 stations, only 39 were selected for the validation purposes (see Table 1 and Figure 2 black dots). The selection process was based on a multi-criteria analysis of each station regarding the length of the time series analyzed, consistency with neighboring stations as well as the distance between two neighboring stations. In order to keep independent of the validation process, the selection process did not involve any prior comparison with model. To provide a quantitative assessment of the model performance, the misfit or RMS error (s) for a single constituent at a single location is defined as the difference in the complex form (z) of the amplitude (A) and phase (G) obtained from the observation (shown with subscript obs) and the model (shown with subscript mod), as shown in equation (2). A misfit gives at single location a quantitative estimate of the combined amplitude and phase difference between model and observation. The equation (3) gives the error associated with a single site (σ_{site}) from the sum of the variance error of each constituent. The error associated with a given constituent ($\sigma_{constituent}$), as shown in equation (4), is given by the mean variance error over all different sites. Finally the Root Sum Square (hereafter RSS) is a combination of the misfits for all sites and all constituents following the equation (5). Then RSS gives a quantitative estimate of the accuracy of a model against an in situ dataset for a given number of constituents.

$$\sigma = \sqrt{\frac{1}{2}|\Delta z|^2} \quad ; \quad |\Delta z|^2 = \left|A_{obs}e^{G_{obs}} - A_{mod}e^{G_{mod}}\right| \qquad (2)$$

$$\sigma_{site} = \sqrt{\frac{1}{2}\sum_{constituents}|\Delta z|^2} \qquad (3)$$

$$\sigma_{constituent} = \sqrt{\frac{1}{2N_{site}}\sum_{site}|\Delta z|^2} \qquad (4)$$

$$RSS = \sqrt{\frac{1}{2N_{site}}\sum_{site}\sum_{constituents}|\Delta z|^2} \qquad (5)$$

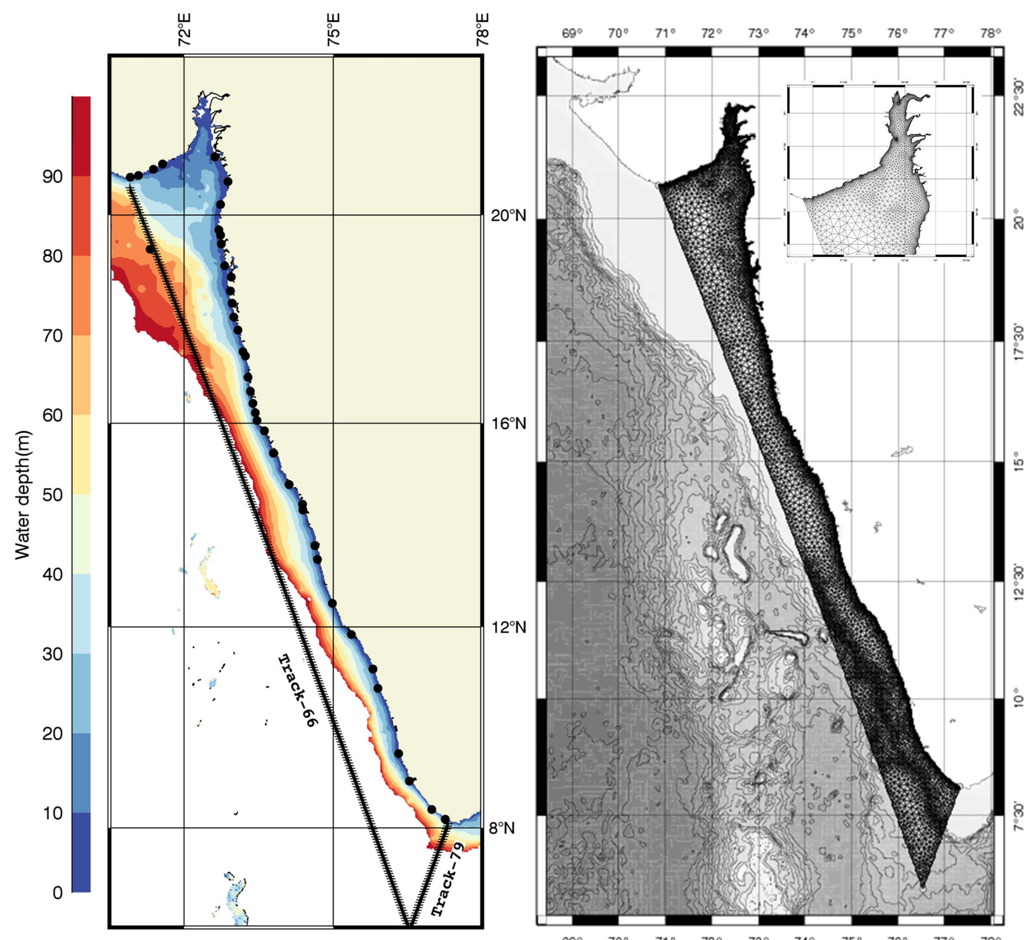

Figure 2: The left panel shows depth contour of the inner shelf bathymetry (0-100 m). The black dot indicates the position of tide gauges used for validation. The two tracks (66 and 79) used as boundary conditions are shown. Right panel shows the model mesh along the west coast of India. The embedded upper right panel is a zoom of the mesh inside the Gulf of Khambhat. The spatial resolution of the mesh ranges from less than 1 km at the coast to a maximum of 20 km in the open ocean. Bathymetric features outside the model domain are also shown

Results

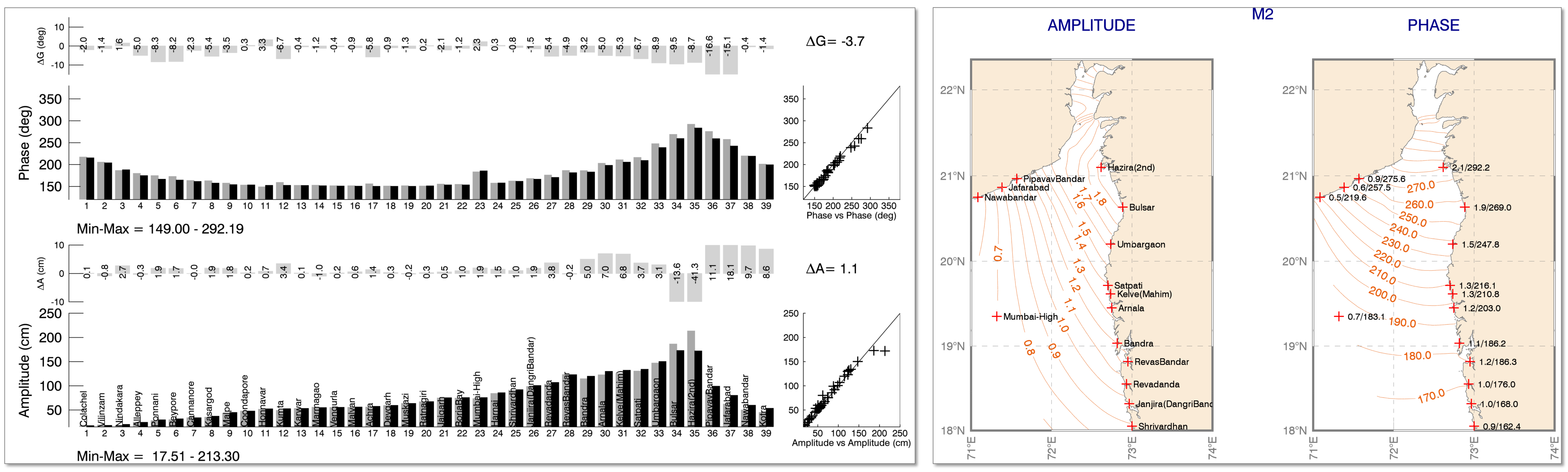

Figure 3: Left panel ➔ comparison for the 39 validation sites ordered along the coast from South (station no.1) to North (station no.39) between the model (black) and the observation (grey). The two upper plots are for the phases (G) and phase differences (ΔG) in degrees and the two lower ones show amplitudes (A) and amplitude differences (ΔA) in cm. The right panels are the corresponding scatter plots for amplitude and phase respectively. All phases are referred to as Greenwich meridian Time, GMT.
Right panel ➔ Map of amplitude A (left panel) and phase G (right panel) of the M2 constituent of the model in the region of the Gulf of Khambhat. The contours indicate amplitude in meter on the left panel and the phase in degree on the right panel. Location and name of the used tide gauge are shown in the left panel and their observed amplitude/phase in the right panel (in the same units as the contour lines).

N	TG	M2	S2	N2	K2	K1	O1	P1	Q1	M4	σ_{site}
1	Colachel	0.4	0.5	1.1	0.5	1.3	0.4	0.5	0.1	0.3	2.0
2	Vilinzam	0.7	2.3	1.1	0.1	0.3	0.6	0.5	0.1	0.4	2.8
3	Nindakara	2.0	3.3	1.4	0.4	2.7	1.8	0.7	0.8	0.4	5.3
4	Alleppey	1.5	1.4	0.8	0.6	1.2	1.3	1.3	0.5	--	3.2
5	Ponnani	3.2	1.7	1.2	0.4	0.9	1.4	3.6	0.4	--	5.6
6	Beypore	3.3	1.1	0.7	1.0	1.2	1.4	0.8	0.4	0.3	4.3
7	Can0ore	1.0	1.3	2.6	0.4	3.9	1.0	1.4	0.3	0.2	5.3
8	Kasargod	2.8	1.9	1.0	0.3	0.8	1.3	0.6	0.3	0.2	3.9
9	Malpe	2.3	0.9	0.9	0.2	0.9	1.2	0.2	0.2	0.9	3.1
10	Coondapore	0.2	0.9	1.0	--	2.4	0.5	--	0.9	0.5	2.9
11	Honnavar	2.2	1.8	1.3	--	1.8	0.8	--	0.3	0.6	3.7
12	Kumta	4.9	2.5	1.9	0.8	0.5	0.7	1.2	0.5	0.4	6.1
13	Karwar	0.3	0.4	0.3	0.4	0.2	0.7	0.2	0.3	0.5	1.1
14	Marmagao	1.1	0.1	0.7	0.1	0.4	0.6	0.1	0.7	0.1	1.6
15	Vengurla	0.3	0.9	1.2	0.3	0.5	0.6	0.9	0.5	0.3	2.0
16	Malvan	0.8	1.1	1.0	0.7	1.2	0.6	1.0	0.5	0.4	2.5
17	Achra	4.2	2.2	1.9	0.9	0.9	1.5	0.9	0.5	1.1	5.6
18	Devgarh	0.7	1.1	0.8	0.9	0.8	0.1	1.0	0.1	0.3	2.2
19	Muskazi	1.0	0.8	0.7	0.5	2.2	0.8	1.7	0.4	0.4	3.3
20	Ratnagiri	0.2	0.4	0.2	0.2	1.1	0.7	0.8	0.4	0.6	1.7
21	Jaigarh	2.0	1.3	1.2	1.0	0.7	0.8	1.1	0.6	0.3	3.3
22	BoriaBay	1.3	1.4	1.9	1.0	0.8	0.5	1.0	0.2	0.4	3.2
23	Mumbai-high	2.5	2.5	2.3	--	3.2	0.9	--	--	--	5.4
24	Harnai	1.1	0.7	1.8	1.0	2.2	0.5	1.4	0.1	0.4	3.6
25	Shrivardhan	1.2	1.0	1.0	1.0	3.4	0.4	2.1	0.5	0.6	4.6
26	Janjira	2.3	1.3	1.9	1.1	5.6	1.1	2.8	1.0	1.4	7.4
27	Revadanda	7.5	3.4	2.2	1.9	4.8	0.3	2.6	0.4	1.5	10.4
28	RevasBandar	7.5	5.3	1.5	2.6	2.1	1.4	1.3	0.4	4.2	10.9
29	Bandra	5.9	3.7	0.9	1.4	2.2	0.5	1.3	0.4	1.4	7.7
30	Arnala	9.2	3.4	2.3	1.6	2.2	0.7	1.4	0.5	1.0	10.7
31	Kelve(Mahim)	9.7	3.1	2.0	1.9	3.9	0.4	1.9	1.3	1.1	11.5
32	Satpati	11.3	3.5	4.9	1.9	5.3	0.6	2.6	1.1	0.2	14.3
33	Umbargaon	16.5	3.2	5.0	2.0	9.4	3.6	3.6	2.2	3.7	21.1
34	Bulsar	23.1	7.0	7.5	2.6	18.1	2.6	7.2	2.1	3.8	32.4
35	Hazira(2nd)	35.7	7.8	7.3	3.3	20.1	7.5	7.0	2.8	2.1	43.9
36	PipavavBandar	20.6	2.6	--	--	5.6	1.3	--	--	--	21.6
37	Jafarabad	18.3	5.1	5.3	1.5	3.5	1.0	2.0	0.2	2.5	20.4
38	Nawabandar	6.9	2.1	2.6	0.9	2.5	1.2	1.9	1.0	0.9	8.5
39	Kotra	6.1	4.4	4.0	0.9	2.1	3.3	1.6	0.8	0.7	9.6
	$\sigma_{constituent}$	9.5	2.9	2.6	1.2	5.2	1.7	2.2	0.9	1.4	RSS=12.0

Table 1: Tidal misfits (cm), as defined in the text, between model and observation. Misfits are given for the 39 selected tidal gauges and the principal tidal constituents. The first row is the station number as indicated on Figure 3.

Figure 3 shows a comparison of the amplitude and phase of the semi-diurnal wave M2 with those obtained from model. It can be seen that the amplitudes increase gradually northward, from about 0.2 m at the southernmost station, Colachel (station no.1) to about 2 meters at Satpati (station no. 32), located at the entrance of the Gulf of Khambhat. The maximum semi-diurnal signal of the model is seen on the west side of the Gulf between Bulsar and Hazira. Table 1 summarizes the RMS misfits between the model simulation and the observations. The overall T-UGOm model RSS error is 12 cm.

		RSS Misfits (cm)		
MODEL		Full data set	South	North
		no. 1-39	no. 1-20	no. 21-39
T-UGOm		12.0	3.7	16.8
GOT4.7		20.8	3.7	29.6
FES2012-HYDRO		21.0	4.8	29.7
TPXO7.2		23.1	4.0	32.8
FES2004		49.3	5.5	70.3

In order to assess the improved performance of the regional model, we applied the same in situ validation using the main available global tidal atlases (GOT4.7, FES2004, FES2012, TPXO7.2). It is found that GOT4.7 is the best available global tidal solution for this region. The global hydrodynamic version of FES2012 does not improve global tidal solution in this region when compared to earlier version, despite the fact that it incorporated the improved bathymetry of Sindhu *et al.* (2007). FES2004 is suspected to have assimilated tide gauges with phase errors in the west coast which could probably explain its low performance in the region. It can be noticed (Table 2) that significant improvement in the performance of the present regional model is found on the northern part of the shelf (from stations no. 21 to 39), where large tidal amplitudes occur (see Figures 7 and 8). Due to the increase in mesh resolution, improved bathymetry, accurate boundary conditions and choice of appropriate bottom friction, the errors in the simulations of the regional model have been considerably reduced.

The present study illustrates the need for developing high-resolution regional tidal models for the north Indian Ocean, for providing accurate tidal corrections for processing altimetric data to generate sea-level anomalies. This becomes important in the context of current SARAL/Altika and future SWOT missions. One of the possible options is to use the altimetry tracks as an open boundary condition for developing regional models, which will permit to prescribe the boundary conditions from the tidal information derived from 20 years of altimetry. This approach was particularly useful in the present case where one of the track is parallel to the isobaths on a shelf where strong amplification of semi-diurnal tides occurs.

Acknowledgments. *This research was supported by the French National Space Agency (CNES) in the frame of the European Organization for the Exploitation of Meteorological Satellites (EUMETSAT) and CNES joint Ocean Surface Topography Science Team (OST-ST) Project. Altimetry data used in this study were developed, validated, and distributed by the CTOH/LEGOS, France. The authors thank Prakash Mehra for providing tidal constituents from recent measurements of NIO.*